

it is reasonable to assume that the two terms of Eq. (9) arise from different physical processes. As it has been already pointed out, the constant B is almost equal to the factor $n_0 M^2 / \rho V^2$ of Eq. (3) for soda silica and Pd-Si. So the second term of Eq. (9) may result from the resonant interaction between the ultrasonic wave and the two-level systems. The last point but not the least is that the first term of Eq. (9) does not seem to be a relaxation term. It gives a large variation of the sound velocity (in comparison with the variation of the sound velocity in crystals in the same temperature range), and may be due to the strong anharmonicity of the disordered lattice.

The author is indebted to Professor J. Friedel, R. Maynard, H. Ishii, and J. Szeftel for enlightening discussions.

¹L. Piché, R. Maynard, S. Hunklinger, and J. Jäckle, *Phys. Rev. Lett.* **32**, 1426 (1974).

²G. Bellessa, P. Doussineau, and A. Levelut, *J. Phys. (Paris) Lett.* **38**, L65 (1977).

³G. Bellessa, C. Lemerrier, and D. Caldemaison, *Phys. Lett.* **62A**, 127 (1977).

⁴J. T. Krause, *Phys. Lett.* **43A**, 325 (1973). In Fig. 1 of this paper it appears that the velocity decreases

linearly as the temperature increases up to 30 K, but it is not the object of the paper and the author does not discuss this variation.

⁵See, for example, G. A. Alers, in *Physical Acoustics*, edited by W. P. Mason (Academic, New York, 1966), Vol. IV, part A, p. 277.

⁶J. Jäckle, *Z. Phys.* **257**, 212 (1972).

⁷J. Jäckle, L. Piché, W. Arnold, and S. Hunklinger, *J. Non-Cryst. Solids* **20**, 365 (1976).

⁸The exact compositions of the soda silica and of Pd-Si are $(\text{Na}_2\text{O})_{0.3}(\text{SiO}_2)_{0.7}$ and $\text{Pd}_{0.775}\text{Si}_{0.165}\text{Cu}_{0.06}$, respectively. The author is indebted to J. Szeftel and O. Bethoux for kindly supplying samples.

⁹G. Bellessa and O. Bethoux, *Phys. Lett.* **62A**, 125 (1977).

¹⁰P. W. Anderson, B. I. Halperin, and C. Varma, *Philos. Mag.* **25**, 1 (1972).

¹¹W. A. Phillips, *J. Low Temp. Phys.* **7**, 351 (1972).

¹²H. Ishii, private communication.

¹³B. Golding, J. E. Graebner, and A. B. Kane, *Phys. Rev. Lett.* **37**, 1248 (1976).

¹⁴S. Hunklinger and W. Arnold, in *Physical Acoustics*, edited by W. P. Mason and R. N. Thurston (Academic, New York, 1976), Vol. XII, p. 155.

¹⁵O. L. Anderson and H. E. Bömmel, *J. Am. Ceram. Soc.* **38**, 125 (1955).

¹⁶P. W. Anderson, *J. Phys. (Paris), Colloq.* **37**, C4-339 (1976).

¹⁷K. F. Herzfeld and T. A. Litovitz, *Absorption and Dispersion of Ultrasonic Waves* (Academic, New York, 1959), p. 135.

Stimulated Phonon Emission

W. E. Bron and W. Grill

Indiana University, Bloomington, Indiana 47401

(Received 14 March 1978)

Inversion, through direct absorption of far-infrared laser light, of a three-level electronic system of V^{4+} ions in dilute solution in Al_2O_3 leads to stimulated emission of 24.7-cm^{-1} phonons. Stimulated phonon emission manifests itself in the presence of ballistic flow of longitudinal phonons along the c axis of Al_2O_3 , but this flow is not observed under spontaneous phonon emission.

We report direct observation of the stimulated emission of 24.7-cm^{-1} (0.74 THz) phonons. Stimulated phonon emission is achieved by inversion of a three-level electronic system of V^{4+} ions in Al_2O_3 and is detected through an analysis of the time-of-flight spectrum of the phonon propagation.

The lowest-lying three electronic states of the $3d^1$ configuration of $\text{Al}_2\text{O}_3:V^{4+}$ have been known for some time,¹⁻³ as have the group-theoretic selection rules for electric-dipole transitions among these states.⁴ As indicated in Fig. 1, the ground

state (numbered 1 in the figure) transforms as the $E_{3/2}$ ($A_{3/2}$ in McClure's notation⁴) representation of the C_3 double group; the first excited state (numbered 2) appears at 28.1 cm^{-1} (0.84 THz) above the ground state with a half-width of $\sim 2\text{ cm}^{-1}$ at liquid helium temperature and is known to transform as $E_{1/2}$, and the next excited state (numbered 3), which appears at 52.8 cm^{-1} (1.58 THz) above the ground state with half-width of $\sim 3.5\text{ cm}^{-1}$, also transforms as $E_{1/2}$. Electric-dipole absorptive transitions from the ground state

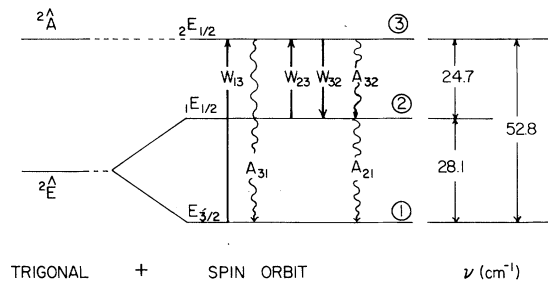


FIG. 1. Energy-level diagram and group-representation assignments for the lowest three levels of the d^1 configuration of V^{4+} in Al_2O_3 , and transition rates.

to the $1E_{1/2}(1 \rightarrow 2)$ and to the $2E_{1/2}(1 \rightarrow 3)$ excited states have been observed by Wong, Berggren, and Schawlow² and confirm the selection rules and polarization requirements for the electric component \vec{E} of an exciting photon field as shown in Table I in which \perp represents \vec{E} perpendicular and \parallel represents \vec{E} parallel to the c axis of the Al_2O_3 crystal. Relaxation of an electron from one of the upper states may occur by emission of either a photon or a phonon. However, since the density of terminal states in the phonon field exceeds that in the photon field by $\sim 10^5$, phonon emission is by far the more likely event.

Following Blume and Orbach,⁵ the rate of spontaneous phonon emission produced by nonradiative decay from the electronic state j to the state i , as given by the orbit-lattice interaction, is

$$A_{ji} = (2\pi/\hbar) \sum_{\Gamma, m} |\langle \psi(\Gamma_i) | V(\Gamma)C(\Gamma, m) | \psi(\Gamma_j) \rangle|^2 \times |\langle n+1 | \epsilon(\Gamma, m) | n \rangle|^2 \rho_E,$$

in which the ψ refer to the initial and final electronic states; ρ_E refers to the density of phonon states at the transition energy $h\nu_{ji}$, and n to the occupation number of phonons of that energy $V(\Gamma)C(\Gamma, m)$ is an orbital operator which transforms as the m th component of the Γ th representation of the point group of the V^{4+} ion site, and $\epsilon(\Gamma, m)$ is the strain associated with a phonon, which transforms in the same way as the orbital operator. From this it can readily be shown that

TABLE I. Selection rules for photon absorption and phonon emission.

	$E_{1/2}$	$E_{3/2}$
$E_{1/2}$	$\perp + \parallel$	\perp
$E_{3/2}$	\perp	\parallel

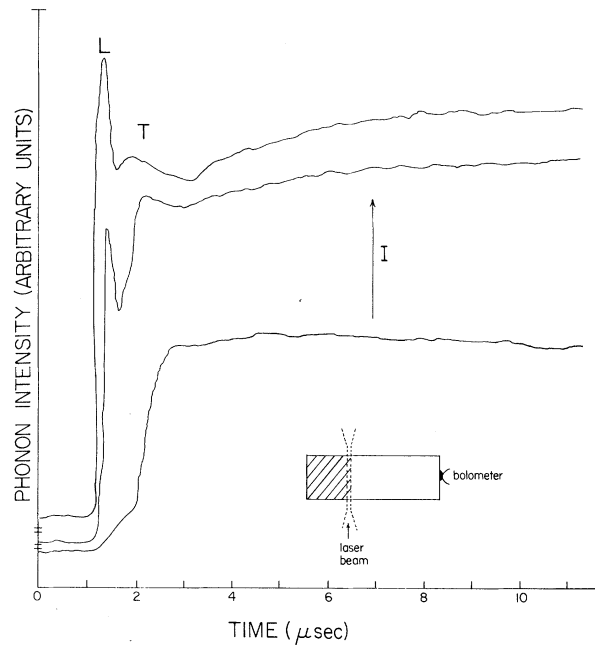


FIG. 2. Phonon intensity, as measured at the bolometer, as a function of elapsed time after the onset of the laser pulse and as a function of laser intensity. The phonon signal is shown in terms of an arbitrary linear scale. The laser intensity, I , increases relative to the bottom curve as 1:1.9:2. The three curves have been arbitrarily displaced from each other. The inset shows the sample and laser beam geometry.

only the transitions $3 \rightarrow 2$ or $2 \rightarrow 3$ can couple phonons with strain components perpendicular and parallel to the c axis, whereas the other transitions can couple phonons with components *only* perpendicular to the c axis. In other words, Table I gives the selection rules for both photon absorption and (one-) phonon emission.

We have observed⁶ phonon emission when far-ir laser light is absorbed by the crystal as described below. A partially doped crystal of Al_2O_3 was purchased from Hrand Djvahirdjian.⁷ The sample was polished to a rectangular shape roughly $0.7 \text{ cm} \times 0.7 \text{ cm} \times 1.7 \text{ cm}$. The c axis of the crystal corresponds to the 1.7-cm dimension. Approximately one-third of the volume of the crystal is doped with 0.3% (nominally by weight) vanadium (see cross-hatched area in inset of Fig. 2); the remaining part of the sample is undoped. For this concentration, ionizing irradiation converts approximately 5% of the total vanadium to the V^{4+} ionization state,⁸ the remainder being mostly V^{3+} . One face of the sample is attached to a thin-walled cylinder so as to form the bottom of the helium reservoir of an optical Dewar. All other faces of

the sample are in vacuum.

A focused (~ 0.25 mm diam) beam from an optically pumped far-ir laser is used to excite the system. The beam is positioned within the crystal so as to be just inside the doped region and at the interface between the doped and undoped region (see inset to Fig. 2). A 250-nsec (base width), 52.6-cm^{-1} pulse from a CO_2 -laser-pumped CH_3F laser is used to excite the 52.8-cm^{-1} ($E_{3/2} \rightarrow E_{1/2}$; i.e., $1 \rightarrow 3$) absorptive transition. Based on the absorption data of Wong, Berggren, and Schawlow,² and on the steady-state temperature rise of the crystal, we estimate that from 10 to 100 W are absorbed depending on the incident power. The arrival time of the phonons at the undoped end of the crystal is monitored with a Sn superconducting bolometer of 1-mm^2 cross section. Observations are made with the bolometer near its transition temperature (i.e., near 3.7°K).

Phonon signals are not detected if the laser beam is focused in the undoped region of the crystal. In contrast, a signal is observed with 28.8- and 52.6-cm^{-1} laser light focused in the doped region, and provided the electric component is perpendicularly polarized to the c axis.⁶ (Weaker phonon signals are observed if the laser frequency is $< 70\text{-cm}^{-1}$ but outside of the strong 28.1- and 52.8-cm^{-1} absorption bands.) The dependence of the time-resolved signal on the intensity, I , of 52.6-cm^{-1} laser light is shown in Fig. 2. At low intensities only a very small signal arrives at a time interval consistent with ballistic flow of longitudinal phonons ($\sim 1\ \mu\text{sec}$), followed by a sharp onset in the signal consistent with the arrival time for ballistic flow of transverse acoustic phonons ($\sim 2\ \mu\text{sec}$). The signal continues for tens of microseconds indicative of the presence of diffusive phonon flow in addition to the ballistic flow. Increase of the incident light intensity by factors of 1.9 and 2 results in the appearance of an increasingly stronger peak in the ballistic longitudinal phonon region, together with a smaller rise in the peak in the ballistic transverse phonon region.

We consider first the results obtained at low laser intensity. At 3.7°K the thermal populations of the two excited states are $N_{3T} \approx 1 \times 10^{-9} N_0$ and $N_{2T} \approx 9 \times 10^{-6} N_0$, where N_0 is the number of V^{4+} ions in the excited volume of the crystal. So long as the optically induced excitation does not invert the relative populations of the three levels, relaxation is dominated by spontaneous emission of phonons. The latter emission occurs either by the generation of 52.8-cm^{-1} phonons or the gen-

eration of 24.7-cm^{-1} followed by 28.1-cm^{-1} phonons. Little is known about the relative strengths of the pertinent transition matrix elements. Assuming that the matrix element for the transition $3 \rightarrow 1$ approximately equals that of $3 \rightarrow 2$, and following the analysis by Blume *et al.*⁹ for $\text{Al}_2\text{O}_3:\text{Cr}^{3+}$, yields a branching ratio for the transition $3 \rightarrow \frac{1}{3} \rightarrow 2$ of ~ 10 . Since only the 24.7-cm^{-1} phonons from the $3 \rightarrow 2$ transition can contribute a longitudinal component along the c axis, the spontaneous emission signal is dominated by the 52.8-cm^{-1} phonons which travel ballistically at the TA velocity along the c axis. The small, broad signal observed at low intensity in the longitudinal region is composed of the contribution from the small number of 24.7-cm^{-1} phonons and by 52.8- and 28.1-cm^{-1} phonons which travel in directions other than the c axis but within the 30° acceptance angle and for which the selection rules of Table I do not apply.

As the light intensity is increased, it becomes possible to invert the relative populations of the ${}_2E_{3/2}$ and ${}_1E_{1/2}$ states, and thereby produce net stimulated phonon emission between these states. In order to demonstrate this point we make recourse to the level scheme of Fig. 1. We denote spontaneous and stimulated processes by A_{ij} and W_{ij} , respectively, with i and j referring to the level numbers. In the figure, the rate of stimulated absorption of the laser light is given by $W_{1,}$, the rate of spontaneous emission of 52.8-cm^{-1} phonons by A_{31} , etc. If the electron population in the ${}_2E_{1/2}$ state is to exceed the thermal population, the absorbed laser power, P , must exceed the losses out of that state; that is,

$$P = W_{13}N_1h\nu_{13} > A_{31}N_3h\nu_{13},$$

in which we have neglected A_{32} relative to A_{31} because of the branching ratio noted above. Neglecting, in addition, losses out of the ${}_1E_{1/2}$ state, we find that the threshold for inversion is reached when $N_3 = N_{2T}$. The spectral lines for the $1 \rightarrow 3$ and $1 \rightarrow 2$ absorptive transitions have been shown to be homogeneously broadened by Wong *et al.*² as have similar lines¹⁰ for the isoelectronic case of $\text{Al}_2\text{O}_3:\text{Ti}^{3+}$. The linewidth for the $1 \rightarrow 3$ transition implies that $A_{31} \approx 3.3 \times 10^{11}\text{ sec}^{-1}$ which, together with $N_0 \approx 1 \times 10^{16}$, requires that P exceed 31 W, which is in fair agreement with our estimate of the absorbed laser power.

The conditions for sustained inversion are further specified in terms of the rate equations for the number of ions N_i in the i th energy state eval-

uated under steady-state conditions. These are

$$dN_3/dt = 0 = W_{13}N_1 + W_{23}N_2 - (A_{31} + W_{32})N_3, \quad (1a)$$

$$dN_2/dt = 0 = -(W_{23} + A_{21})N_2 + (W_{32} + A_{32})N_3, \quad (1b)$$

$$N_1 + N_2 + N_3 = N_0. \quad (1c)$$

In Eq. (1a) we again neglect A_{32} relative to A_{31} because of the branching ratio, and in Eqs. (1a) and (1b) we neglect W_{31} , W_{21} , and W_{12} because the required inversion is much harder to achieve or the required stimulating field is not present. Equations (1a)-(1c) specify that for inversion, i.e., for $N_3 - N_2 > 0$, it is required that $W_{23} + A_{21} > W_{32} + A_{32}$. Since $W_{ij} = W_{ji}$ when the degeneracies of the two states are equal,¹¹ the requirement reduces to $A_{21} > A_{32}$, a condition which is met in terms of the relevant density of terminal states provided that the transition matrix elements are roughly equal.

The experimental observation that the longitudinal peak in the time-resolved spectrum is narrower than the transverse peak can be understood as follows. If we neglect the small contribution from off-axis ballistic phonons, it is clear from Table I that the L peak comes only from 24.7-cm⁻¹ phonons, whereas the T peak is a superposition of contributions from 52.8-, 28.1-, and 24.7-cm⁻¹ phonons. However, the probability of strong resonant phonon scattering, through reabsorption and reemission at V⁴⁺ ions, is down by the factor $N_2/N_1 \sim 10^{-5}$ for 24.7-cm⁻¹ as compared to 52.8- and 28.1-cm⁻¹ phonons. The 24.7-cm⁻¹ phonons are subjected, therefore, primarily to the weaker, nonresonant elastic scattering at the mass defect which the vanadium ions, regardless of valence, represent. The magnitude of this scattering rate, τ_{NR}^{-1} , is not known except that an analysis⁶ of diffusive phonon flow in this system places it somewhere between the rate of resonant scattering $\tau_R^{-1} \sim 2 \times 10^{10} \text{ sec}^{-1}$ and $\sim 2 \times 10^7 \text{ sec}^{-1}$ found for nonresonant scattering of low-frequency phonon decay products. In order that sufficient interaction exist between the 24.7-cm⁻¹ phonons and the 3 → 1 resonance to cause stimulated emission, we would have to require that $\tau_{NR}^{-1}(24.7 \text{ cm}^{-1}) \sim 10^{-8}$ to 10^{-9} sec^{-1} . In any event τ_{NR}^{-1} , which at fixed phonon frequency varies¹² with the group velocity as $\sim v^{-3}$, is accordingly smaller for longitudinal than for transverse phonons. The broader ballistic T peak arises, therefore, from the enhanced probability for small-number scattering events prior to detection for transverse as compared to 24.7-cm⁻¹ longitudinal, phonons.¹³ Indeed we observe ex-

perimentally that the additional transverse peak smears out faster than the L peak as the excitation volume is moved further into the doped region of the crystal. The strong impurity scattering (plus phonon-phonon scattering⁶) is further evidenced in the strong and prolonged diffusive tail in the time-of-flight spectrum and from the observation that displacement of the excitation volume of less than 0.1 mm into the doped region completely removes the ballistic L and T peaks.

We contend that we have observed stimulated phonon emission of 24.7-cm⁻¹ phonons. On the other hand, we have so far failed to observe an expected anisotropy in the phonon intensity from the geometry of the gain region. An attempt was made to detect a forward directionality in the signal by passing the laser light at various positions parallel to the c axis from the doped end of the crystal toward the bolometer, thus producing a cylindrical excitation volume (gain region) perpendicular to the direction shown in the inset of Fig. 2. Failure to detect a directionality stems in part from saturation of the bolometer by the laser light and possibly from the losses in the gain volume due to defect scattering.

The authors are indebted to J. M. O'Connor for his aid during the early parts of the experimentation and to L. L. Chase and W. L. Schaich for helpful discussions. The work was supported by National Science Foundation Grants No. 72-02070 and No. 76-23571. One of the authors (W.G.) acknowledges a travel grant from the Deutsche Forschungsgemeinschaft.

¹R. M. Macfarlane, J. Y. Wong, and M. D. Sturge, *Phys. Rev.* **166**, 250 (1968).

²J. Y. Wong, M. J. Berggren, and A. L. Schawlow, *J. Chem. Phys.* **49**, 835 (1968).

³R. R. Joyce and P. L. Richards, *Phys. Rev.* **179**, 375 (1969).

⁴D. S. McClure, *J. Chem. Phys.* **36**, 2757 (1962).

⁵M. Blume and R. Orbach, *Phys. Rev.* **127**, 1587 (1962).

⁶J. M. O'Connor, Ph.D. thesis, Indiana University, 1977 (unpublished).

⁷Hrand Djvahirdjian Ltd., Monthey, Switzerland.

⁸A. M. de Goër and N. Devismes, *J. Phys. Chem. Solids* **33**, 1785 (1972).

⁹M. Blume, R. Orbach, A. Kiel, and S. Geschwind, *Phys. Rev.* **139**, A314 (1965).

¹⁰E. D. Nelson, J. Y. Wong, and A. L. Schawlow, *Phys. Rev.* **156**, 298 (1967).

¹¹See, e.g., A. Yariv, *Quantum Electronics* (Wiley, New York, 1975), 2nd ed., p. 185.

¹²P. G. Klemens, in *Solid State Physics*, edited by F. Seitz and D. Turnbull (Academic, New York, 1958), Vol. 7, p. 1.

¹³The difference in the propagation velocities between *L* and *T* phonons and geometric effects do not account for the observed difference in width.

Observation of Nondipole Electron Impact Vibrational Excitations: H on W(100)

W. Ho and R. F. Willis

*Astronomy Division, European Space Research and Technology Centre,
European Space Agency, Noordwijk, Holland*

and

E. W. Plummer

Department of Physics, University of Pennsylvania, Philadelphia, Pennsylvania 19104
(Received 6 March 1978)

High-resolution inelastic electron spectra have been measured for a saturated coverage of atomic hydrogen adsorbed on W(100). The fundamental modes corresponding to H occupying a C_{2v} point-group-symmetry bridge site plus an overtone ($\nu = 0 \rightarrow 2$) of the intense symmetric stretch are resolved at angles off the specular direction. The intensity of these modes (normalized to the elastic peak) exhibits resonantlike behavior as a function of the impact energy.

Traditionally, high-resolution electron-energy-loss spectroscopy studies of the surface vibrations of chemisorbed atoms or molecules have been interpreted in terms of long-range dipole scattering.¹⁻³ The assumption of dipole scattering from an adsorbate on a metal surface leads to the following predictions: The inelastic intensity is strongly localized (within $\sim \pm 2^\circ$) about the specularly reflected beam direction, and only those vibrational modes with a dynamic dipole moment perpendicular to the surface are excited.¹⁻³ The latter consequence of dipole scattering is referred to as the "surface dipole selection rule." It predicts that the relative intensities of the observed vibrational modes in electron scattering should be similar to those observed in an infrared absorption experiment.¹

There is strong evidence supporting this dipole scattering model, especially for adsorption of atomic hydrogen on tungsten. The inelastic spectra for hydrogen adsorbed in all of the high-symmetry sites—on-top, bridge, or four-centered sites—exhibit only a single energy loss which is associated with the excitation of the stretching mode perpendicular to the surface.⁴ All of these measurements were taken in the specular beam direction, where the dipole scattering cross section is the largest. In this Letter, we show that all of the fundamental modes relating to H occupying a C_{2v} point-group-symmetry bridge site [see

inset, Fig. 1(b)] can be observed when the measurements are made off the specularly reflected beam direction. The scattering mechanism is clearly nondipole as witnessed by the observation of modes which are forbidden by the "surface dipole selection rule," by the observation of an overtone mode and by the large momentum transfer associated with collection angles far from the specular direction.

Figure 1(a) shows a typical electron-energy-loss spectrum for hydrogen chemisorbed on W(100) at saturation coverage (β_1 phase, 2×10^{15} atoms/cm²),⁵ in the *specular direction* for an impact energy $E_0 = 9.65$ eV and an angle of incidence $\theta_i = 23^\circ$.⁶ A single loss at $h\nu_1 = 130$ meV is observed and corresponds to the symmetric stretch vibration normal to the surface (A_1 mode).⁷ Previous measurements^{8,9} have reported the single loss peak at 130 meV and much weaker loss peaks at 70 meV⁸ and 79 meV.⁹ The low-energy losses were attributed to CO contamination⁸ or a "bending mode" of the β_2 (low-coverage on-top site) H phase. In contrast to the spectrum shown in Fig. 1(a), taken in the specular direction, Fig. 1(b) shows that off the specular direction a multitude of modes are observed (80, 130, 160, and 260 meV). This spectrum was taken under the same incident-beam and hydrogen-adsorption conditions. The 160-meV peak is clearly resolved at other angles of incidence and collection.¹⁰ All